1-1-2014

The Impact of pH on the Structure and Function of Neural Cadherin

Jared Michael Jungles
University of Mississippi

THE IMPACT OF PH ON THE STRUCTURE AND FUNCTION OF NEURAL CADHERIN

A Thesis
presented in partial fulfillment of requirements
for the degree of Master of Science
in the Department of Chemistry and Biochemistry
The University of Mississippi

by

JARED JUNGLES

July 2014

ABSTRACT

Neural (N-) cadherin is a transmembrane protein within adherens junctions that mediates cell-cell adhesion. It has 5 modular extracellular domains (EC1-EC5) that bind 3 calcium ions between each of the modules. Calcium binding is required for dimerization. N-cadherin is involved in diverse processes including tissue morphogenesis, excitatory synapse formation and dynamics, and metastasis of cancer. During neurotransmission and tumorigenesis, fluctuations in extracellular pH occur, causing tissue acidosis with associated physiological consequences. Studies reported here aim to determine the effect of pH on the dimerization properties of EC1-EC2 N-cadherin in vitro. Since N-cadherin is an anionic protein, we hypothesized that acidification of solution would cause an increase in stability of the apo protein, a decrease in the calcium-binding affinity and a concomitant decrease in the formation of adhesive dimer. The stability of the apo monomer was increased, and the calcium-binding affinity was decreased at reduced pH, consistent with our hypothesis. Surprisingly, analytical SEC studies showed an increase in calcium-induced dimerization as solution pH decreased from 7.4 to 5.0. Salt-dependent dimerization studies indicated that electrostatic repulsion attenuates dimerization affinity. These results point to a possible electrostatic mechanism for moderating dimerization affinity of the Type I cadherin family.

DEDICATION

This thesis is dedicated to my family who have pushed and encouraged me to strive for success.

ABBREVIATIONS

Apo, Calcium-depleted

CD, Circular dichroism

EC, Extracellular domain

EC1, Extracellular domain 1 of NCAD12

EC2, Extracellular domain 2 of NCAD12

EDTA, Ethylenediaminetetraacetic acid

HEPES, N-(2-hydroxyethyl) piperazine-N'-2-ethanesulfonic acid

K_a, Acid Dissociation Constant;

K_d, Dissociation constant;

NaOAc, Sodium Acetate

NCAD12, Neural-cadherin extracellular domains 1 and 2 (residues 1 to 221)

ECAD12, Epithelial-cadherin extracellular domains 1 and 2 (residues 1 to 213)

PAGE, Polyacrylamide gel electrophoresis

SEC, Size exclusion chromatography

T_m, Melting temperature

TABLE OF CONTENTS

LIST OF TABLES

LIST OF FIGURES

CHAPTER I

Chapter 1 of this thesis contains a brief review of cadherin structure and function with special attention paid to the unique physiological responsibilities of neural cadherin. The use of PROPKA for estimation of pKa of ionizable amino acid residues will be discussed as well.

INTRODUCTION

Solid tissue requires adhered cells. Adhesion occurs in several varieties including tight junctions, adherens junctions, and desmosomes, all of which require transmembrane proteins called cell-adhesion proteins. Among the family of these cell adhesion proteins, the cadherin family has 6 sub families with a total of over 100 known members that are differentially expressed according to tissue type and organism [1]. Cadherins are transmembrane proteins with dynamic, extracellular domains whose interactions with apposing cells facilitate specific cell response mechanisms [2]. They are calcium-dependent glycoproteins whose homophilic interactions form adherens junctions between cells [3]. The responsibility of cadherin in maintaining multicellular structure integrity [4], selecting cell-cell adhesion (cell sorting) [5], and playing important roles in embryogenesis has been widely studied [6, 7]. Cadherins bind to α- and β-catenins in the cytoplasm to form the cadherin/catenin complex to link cellular adhesion to intra-cellular signaling pathways including gene expression and cell cytoskeleton activation. Considering the vast location and cellular implications of cadherin molecules, understanding how environmental fluctuations affect their structure and function can be useful.

STRUCTURE

In terms of structure, all members of the cadherin family are similar, with an extracellular, multi-domain β-barrel structure with an IgG type I consensus fold [8]. The extracellular (EC) region is anchored to the cell membrane via a short transmembrane region (approximately 24 residues) followed by another short cytoplasmic region that is highly conserved across the cadherin family. Each EC domain consists of seven (A-G) β-strands that are structurally similar across the cadherin family, with the exception of the strand A in EC1, which participation in adhesive dimer formation. These EC domains consist of approximately 110 amino acid residues. A hydrophobic pocket is located in EC1 that allows docking of strand A from a partner protomer. This pocket consists of hydrophobic residues involved in the interaction between a tryptophan residue (W2) during the "closed" monomer state, as well as the strand-swapped dimer state. The "open" monomer state describes the condition where strand A is exposed and W2 is accessible to solvent. This tryptophan docks in the hydrophobic pocket, which contains hydrophobic residues, most notably an alanine (A80), whose methyl side chain is thought to interact with W2 [9-11]. A mutation of W2, as well as A80, results in a loss in dimerization capability [10]. A multi-proline sequence in strand A allows for a decrease in hydrogen bonding with strands B and G, and is responsible for the increase in strand mobility required for dimerization [12, 13].

Cadherins form several dimer structures that are physiologically relevant. Dimerization affinities are dependent on calcium concentration, and can differ through the cadherin family [14, 15]. Three calcium ions bind in conserved sites between each EC domain. The N-terminal, extracellular domain engages in dimerization with a partner protomer via a β-strand, strand cross-over mechanism (strand-swapped dimer). Dimerization is achieved through an

intermediate state called the initial-encounter complex (X-dimer) before the strand-swapped dimer conformation is formed. This X-dimer interface is located in the EC1 domain, opposite the strand-swapped dimer interface. Dimerization causes a shift from a dynamic to a more rigid structure; a process that is thought to have one or more intermediary structures [16]. Some members of the cadherin family can undergo lateral (cis) dimerization, thought to increase adhesivity and promote trans dimerization. Whereas trans dimerization occurs between two protomers emanating from two different cell surfaces, cis dimerization occurs amongst protomers of a single cell. This cis aggregation can be accomplished as homo or heterodimers [17], a significant difference from the rarity of trans-heterodimerization, which is thought to only occur during tissue remodeling or cell migration [18, 19]. The location of the "cis interface" was found to be between the two domains [20, 21]. Furthermore, a highly conserved HAV sequence (H79, A80, and V81) is essential for trans dimerization and, presumably, the functionality of the hydrophobic pocket [22]. However, mutations in the HAV sequence do not hinder the formation of the cis dimer. Moreover, elucidation of dimerization dynamics and pathways is paramount considering the widespread expression and physiological importance of the type 1 cadherin family.

NEURAL CADHERIN

One of these differentially expressed cadherin is neural cadherin (NCAD), which is expressed in a variety of tissues, notably neuronal synapses [23, 24] and metastatic cancer cells [25, 26]. Concerning neurons, NCAD is involved in synaptic plasticity and dendrite morphogenesis and located primarily at excitatory synapses. Studies have shown that NCAD is specifically expressed in key regions such as synaptic junctions and primordial neural tubes [23, 27]. Recent studies have shown that increased neuronal activity results in increased expression of NCAD on

dendrite cell surfaces[28]. Furthermore, the ability to establish new synaptic connections has been inhibited through NCAD antibodies [29]. NCAD is required for late-phase long term potentiation (LTP), leading to its essential role in memory function [30]. The NCAD-catenin complex has been shown to be involved in processes such as pre and postsynaptic organization and synapse function [27]. In periods of increased synaptic activity, we see a proton influx into the extracellular space. The effect of a decrease in pH on NCAD has only been a topic of recent interest [31]. It should be noted that increased synaptic activity results in a decrease of calcium concentration at the synaptic junction. This same extracellular pH fluctuation is witnessed in metastatic cancer cells.

Along with neurons, NCAD expression is increased in cancer cells consistent with tumor progression and metastasis. The decrease in epithelial cadherin (ECAD) expression and increased NCAD expression (cadherin-switching) consistent in metastasis was found to be a rate limiting step in tumor progression [32-35]. This upregulation of NCAD has allowed the protein to be used as a marker for more aggressive lesions [36, 37]. NCAD is thought to assist cancer cells in adhering to secondary sites in the body by binding to fibroblast growth factor receptor (FGFR) as it does in neuron outgrowth [38]. The binding of NCAD to FGFR elicits a cellular response resulting in the expression of an extracellular matrix degradation enzyme (MMP-9) [39]. The production of MMP-9 is characterized by heightened cellular invasiveness and eventual metastasis [40, 41]. Concerning the extracellular environment in cancer cells, it is known that the EC space in tumors undergo acidification due to protons being pumped out of the cell. Increased metabolic rates cause an increase in protons generated inside tumor cells, which are pumped into the extracellular space by an increase in transmembrane proton pump expression. This “reverse”

pH gradient is a hallmark of most cancer cells, regardless of tissue location (c.f. [42, 43]). The effect of this drop in pH, if any, on cell adhesion by NCAD has not yet been characterized.

Moreover, we see a common theme of extracellular pH decreasing in both the firing of neurons and the metastasis of cancer. The measurement of pH in active synapses has been unsuccessful. The decrease in pH in cancer tissue has been measured to be as low as 6.5 [43] and 5.2 in the extracellular space of synapses [44-46]. The effect of the exposure of NCAD to this pH fluctuation provides a simple question. Does this drop in pH have an effect on the structure or function of NCAD?

EFFECTS OF pH

The activity and function of many proteins are affected by pH through stability, ligand binding, assembly, and dynamics [47-50]. Also, the in-vitro expression of membrane proteins can be affected with fluctuations in extracellular pH [51]. The introduction of hydrogen ions into solution causes protonation of titratable sites which varies the net charge of a protein. This continuously alters the electrostatic environment on the surface of a protein. Electrostatic interactions, such as salt bridges and hydrogen bonding networks, are governed by charged residues. The protonation of titratable residues is governed by the pKa of the side chain groups such as the distal carboxyl groups in aspartate and imidazole groups in histidine residues. The de-protonation of basic residues, arginine and lysine, are possible as well; however, these pKa values tend to stay above physiological pH (7.4-6.8). The pKa values of acidic and histidine residues can shift into the physiological range, leading to their relevancy in governing protein dynamics and interactions.

Residue pKa values can differ based on location, neighboring side chains, and solvent exposure. Isolated acidic amino acid pKa residues exist well outside physiological pH range;

however, when these residues encompass a protein, the free energy of ionization is modified. Buried acidic residues have been shown to have pKa values as high as 9 in some instances [52]. Acidic residues, usually located on the exterior of a protein, can be located in ligand binding pockets, which could make them particularly sensitive to large pKa shifts. The protonation of these ligand-binding residues could affect ligand-binding affinity. Resident side chains can also affect pKa values in acidic residues. Hydrogen bonding with neighboring residues results in a decrease in pKa value from the isolated value [53]. Lastly, acidic residue pKa values can shift as a result of solvent exposure, or lack thereof. Carboxyl groups of acidic residues that are buried in the hydrophobic core of a protein often show increased pKa values. Desolvation decreases the pKa values of basic residues and histidine by increasing the energy of the positively charged acid [54]. Histidine residue pKa values have been shown to be as low as 4.6 and as high as 9.2 [55, 56]. Moreover, histidine residues have been characterized as pH "sensors" concerning protein conformation [57, 58]. All of these factors contribute to shifting pKa values of amino acid residues resulting in the dynamic electrostatic surface of a protein.

COMPUTATION OF pKa VALUES

There are many ways to determine amino acid residue pKa values. Experimental practices such as protein NMR titrations are implemented for the most accurate estimates; however, this method is time consuming and particularly challenging for large, acidic proteins such as cadherin. Computational methodologies can also be utilized to assess pKa values, each method having its own respective advantages and disadvantages. Early methods were based on continuum dielectric models with the assumption that proteins were a low volume, low dielectric constant sphere immersed in a solvent with a high dielectric constant [59]. The simplicity of these methods led to inaccurate results that were improved through modifications such as the

correction for exposed surface area, protein-solvent interface models, and induced charge perturbations. Most computational methods involve solving the Poisson-Boltzmann (PB) equation, which models the total electrostatic surface charge of a protein given charge distribution and dielectric effects [60]. Solving the PB equation is dependent on a static structure that is unrealistic in most cases concerning proteins. Herein lays one disadvantage of the computational method of determining pKa values; the utilization of protein crystallography structures, implying that proteins are static, non-dynamic structures [61]. Also, these methods do not take into account the effect of pH on the structure of a protein. To quantify accuracy, results from studies of model proteins using computational methods are compared to those from experimental methods to determine a root mean square deviation (RSMD). Those methods which have a RMSD <1 are preferred [54, 62].

We implemented an empirical computational method in our work, PROPKA, which has been widely discussed in recent years [63-65]. With a RMSD of 0.78 pKa units, this method is suitable for our studies. PROPKA predicts pKa values of ionizable groups by applying an environmental perturbation to an unperturbed, intrinsic pKa value of that same group. Through hydrogen bonding, desolvation effects, and charge-charge interactions, PROPKA estimates pKa values of titrabable residues in a PDB file [54, 66]. This process becomes problematic with ionizable residues that bind ligands or are deeply buried. Recent advancements incorporated in PROPKA 3.1 have improved the task of estimating pKa value at these sites. PROPKA 3.1 was developed for the purpose of determining the effects of binding of multiple ligands on the pKa values of adjacent ionizable groups. Also, PROPKA 3.1 takes into account covalently and non-covalently coupled ligand groups. Perhaps the largest advantage of PROPKA compared to other

methods is the speed at which results can be obtained. With the selection of a PDB file and PROPKA version, pKa estimations can be obtained in seconds.

ELECTROSTATICS IN NCAD

In our experiments, we use an abbreviated NCAD construct consisting of the two most distal EC domains. NCAD12 is well studied and is determined to be the simplest construct capable of dimerization [9, 67, 68]. Comprising of 219 residues, 24 acidic residues and 15 basic residues, NCAD12 has an overall charge of -8.8 at pH 7.0 [69, 70]. In the folded structure, acidic residues are located on the surface or in the calcium-binding region between EC1 and EC2. There is also a dense population of titratable residues located at the dimerization interface toward the distal portion of EC1. Three histidine residues are located in NCAD12, none of which are located by the calcium-binding cleft or dimerization interface. All three calcium-binding sites are composed of acidic residues. Considering that the residues that bind calcium are relatively buried, we would expect pKa values that are shifted toward a physiological pH. Protonation of these acidic residues could result in different calcium-binding affinities as well as structural consequences. Also, protonation of negatively charged residues on a protomer that is overall negatively charged could result in an increase in stability by reducing electrostatic repulsion. We utilized PROPKA 3.1 to estimate pKa values of all titratable residues in NCAD12 through the 2QVI PDB structure, which includes calcium ions bound. These results point toward a select number of residues that could govern NCAD12 properties. The protonation of acidic and/or histidine residues resulting from decreasing solution pH showcase how the electrostatic properties of a protein can shift and affect protein properties.

We assessed NCAD12 stability, calcium-binding affinity, and dimerization affinity as a function of pH. We hypothesized that a decrease in pH would result in an increase in NCAD12

stability due to a decrease in a net negative charge at pH 7.4. In addition to stability, we would expect the calcium-binding affinity to decrease due to the protonation of calcium-binding residues. Lastly, due to a decrease in calcium-binding affinity, we would expect a decrease in dimerization affinity. Results of these hypotheses are outlined in the next chapter.

CHAPTER II

Chapter II contains a submitted manuscript detailing all experimental procedures, results, and a limited discussion. The manuscript is entitled, *Impact of pH on the Structure and Function of Neural Cadherin.* This paper was submitted to *ACS Biochemistry*. It is currently under revision. Matthew Dukes is second author and was an active participant in aspects of data collection and initial discussion of concepts. I was directly responsible for all data in figures, tables, and all computational efforts. I also wrote and revised this manuscript.

INTRODUCTION

Extracellular pH in humans is actively maintained between pH 7.2 and 7.4, except in abnormal states such as metastatic cancer [71, 72], unregulated diabetes mellitus [73, 74], starvation [75], and extreme synaptic activity, where pH has been shown to be as low as pH 6.0 [76]. The effect of the microenviroment on cell-cell adhesion may play a significant physiological role. Our interest is in how decreased pH will affect adhesion by N-cadherin, a cell adhesion molecule in adherens junctions that is critical in neurological synapse formation [77, 78]. N-cadherin is the primary cell adhesion protein within synaptic adherens junctions at the transmission zone, and is directly exposed to proton flux during periods of increased synaptic activity [45]. N-cadherin expression is also up-regulated in tumor progression, angiogenesis, and metastasis of numerous

types of cancer cells [26, 79-81]. Tumors in active periods of growth have been shown to acidify due to the Warburg effect, a state that is consistent with tumor cell proliferation [82, 83]. Since N cadherin is an anionic protein, pH may have a profound effect on its structure, stability, and function.

N-cadherin is a member of the classical or type I cadherin family consisting of five tandem repeating extracellular domains, a single-pass transmembrane region, and a conserved C-terminal cytoplasmic region [84]. Formation of adhesive dimers between cadherins on apposing cell surfaces occurs through the formation of a strand-swapped structure, which forms via the exchange of the N-terminal βA-strand between juxtaposed EC1 domains [3, 5, 85]. The strand-swapped structure is stablilized by docking of the side chain of a conserved tryptophan (W2) into the conserved hydrophobic pocket of the neighboring protomer. Since the strand-swapped interface is located in the first domain of the EC region [21, 86, 87], the studies reported herein utilize the first two EC-domains of N-cadherin (NCAD12). The two-domain construct has been well characterized in Type I cadherins [9, 67, 88] and is the minimal functional unit required for calcium-dependent dimerization in vitro.

The interface between tandem EC domains contains amino acids that play critical roles in the adhesion process. These amino acids constitute three calcium-binding sites composed of clusters of negatively-charged carboxyl groups from both modular domains that comprise the calcium-binding pocket. The critical anionic residues in the NCAD12 calcium-binding pocket are E11, D67, E69, D103, D134, D136 and D194 in N-cadherin. Calcium-binding sites 1 and 2 are linked by the side chain oxygens of E11, E69, and D103. Sites 2 and 3 are linked by the side chain oxygens of D136, while site 3 comprises, in part, both side chain oxygens from D134 [67].

Studies have shown that mutations of these residues resulted in a dramatic decrease in calcium-binding affinity and dimerization [10, 89, 90].

Isolated amino acid pK_a values of acidic residues (4.5-3.3) are well outside the physiologicially relevant range (7.4-6.0) [91]; however, K_a values for acidic residues in folded proteins can differ by orders of magnitude from these canonical values, especially in acidic proteins where they have been shown to be as low as 10^{-9} [92-94]. NCAD12 also contains three histidine residues (H75, H79, and H110) whose protonation state would change in a physiological relevant pH range. Histidine residues have been characterized as "pH sensors" [57, 58, 95], and can affect protein conformational stability in a physiological pH range [96]. Thus, we might expect significant protonation of critical acidic and histidine residues in a physiologically relevant pH range.

Since the residues comprising the calcium binding sites are highly anionic, we hypothesized that a decrease in solution pH would stabilize NCAD12 due to the decrease in electrostatic repulsion from neutralization of acidic residues. We also hypothesize that an increase in solution acidity would introduce competition between calcium and protons for site occupancy, resulting in a reduction of calcium-binding affinity followed by a concomitant decrease in dimerization affinity. In this work, we will address the impact of pH on the stability, calcium-binding affinity, and the dimerization affinity of NCAD12 protomers using spectroscopic and chromatographic methods.

EXPERIMENTAL PROCEDURES

Protein Expression and Purification

The cloning of the gene for the first two extracellular domains (residues 1-221) of NCAD12 (EC1, linker1, EC2, and linker2) was described previously [97]. Recombinant pET30 Xa/LIC plasmids were amplified by KOD HiFi DNA Polymerase (Stratagene) and transformed into *Escherichia coli* BL21 (DE3) cells [97]. Protein was overexpressed and purified as described in previous work [98]. Protein purity was verified via SDS-PAGE in 17% Tris-Glycine gels through standard protocol [99]. The concentration of the protein stocks was determined spectrophotometrically (ε_{280} = 15,900 ± 400 $M^{-1}cm^{-1}$) [100].

Dilution Method for pH Adjustment

In order to create protein solutions at a range of pHs (7.4-5.0), we prepared our stock at pH 7.4, but with a low buffer strength (2 mM HEPES). Identical diluent buffers at higher buffer strength were made at pHs 7.4, 7.0, and 6.5 (40 mM HEPES, 140 mM NaCl) and at pH 6.0, 5.5, and 5.0 (40 mM NaOAc, 140 mM NaCl). The NCAD12 stock in 2 mM HEPES at pH 7.4 was diluted 1 part protein stock plus 2.4 parts diluent buffer (e.g. 80 μM stock; 23.5 μM working concentration). We confirmed that this dilution ratio was sufficient to adjust the pH to the desired level by measuring pH with a microelectrode.

Thermal Unfolding Studies

Thermal unfolding studies as a function of calcium and pH (6.0, 6.5, 7.0, and 7.4) were performed on an AVIV 202SF Circular Dichroism (CD) Spectrometer. Solutions of 5 μM NCAD12 were placed in a 1 cm quartz cuvette with a fitted temperature probe inserted through the stopper. This concentration was chosen to minimize dimer formation while maximizing signal to noise. The solution was stirred throughout data acquisition. Data were acquired at 227

nm at a temperature range of 15-95 °C (1°C intervals with a 30 sec equilibration period and a 5 sec data averaging time). The calcium-saturated samples were brought to 2.5 mM total calcium concentration to ensure maximum saturation of binding sites at all pH values. Data were fit to the Gibbs-Helmholtz equation with linear native and denatured baselines as described previously [101]. T_m and ΔH_m values were allowed to vary in fits to this equation, while ΔC_p was fixed to 1 kcal mol^{-1} K^{-1}[97]. ΔC_p was also fixed to 0 kcal mol^{-1} K^{-1} and 2 kcal mol^{-1} K^{-1} to determine the effect of its value on resolved values of ΔH_m and T_m. Variation, as a function of the value for ΔC_p, was smaller than the standard deviation in the resolved parameters.

Calcium Titrations

The CD signal of NCAD12 was monitored during calcium titrations using an Olis DSM 20 CD Spectrometer. Solutions of 1 mM, 10 mM, 100 mM, and 700 mM $CaCl_2$ were each added sequentially in 2.5 µL, 5.0 µL, and 10.0 µL increments to 5 µM NCAD12 in solutions with pHs between 7.4-5.5. Samples were stirred throughout the titration. Titrations were performed at least twice. CD signal was recorded in wavelength scans from 300-210 nm with an averaging time (1-13 seconds) that was proportional to dynode voltage at each wavelength. To resolve free energy changes for calcium binding, titration data were considered at wavelengths from 230-220 nm to optimize the signal to noise ratio. Titration data were fit to an equation for equal and independent sites with linear apo and saturated baselines. While we expected cooperative binding of calcium, data did not support analysis by a more complex model based on the span and randomness of residuals of fitted data.

Disassembly and Assembly Studies

The impact of pH on dimer formation was investigated using Size Exclusion Chromatography (SEC). A Superose-12 10/300 GL column (Amersham) was used on an ÄKTA

Purifier HPLC system (Amersham) with UV absorbance detection at 280 nm, a 0.5 mL/min flow rate, and a 75 µL injection volume. The mobile phase consisted of 10 mM HEPES, 140 mM NaCl, pH 7.4 (SEC Buffer). Chromatograms were offset corrected and then normalized against the total height of the monomer and dimer peaks in the pH 7.4 sample to correct for small differences in injection volume.

To determine the effect of pH on the assembly of dimer in the presence of calcium, we exploited an analytically useful property of NCAD12. That is, rapid decalcification of the calcium-saturated NCAD12 dimer (D_{sat}) causes the formation of a kinetically-trapped dimer (D^*_{apo}). In this method, the concentration of D^*_{apo} reflects the amount of D_{sat} in the calcium-saturated solution [98]. To measure the effect of pH on the formation of D_{sat}, we first assessed the effect of pH on D^*_{apo}. Secondly, we determined the effect of pH on D_{sat}.

To determine if pH had an effect on the disassembly of D^*_{apo}, the protein stock (80 µM, pH 7.4) was brought to 1 mM calcium concentration and incubated for 5 minutes before adding EDTA (5 mM, 30 minute incubation time) to decalcify and convert D_{sat} to D^*_{apo}. The dilution method outlined above was used to bring the protein to a desired pH, and samples were injected on the SEC column equilibrated in SEC buffer (pH 7.4) to assess the level of monomer and dimer. To observe if disassembly of D^*_{apo} was time dependent, samples were incubated after dilution to the desired pH for 0, 1 and 5 hours before injecting on the column.

To assess whether pH had an effect on the level of D_{sat}, we first established that D^*_{apo} did not disassemble at pH lower than 7.4. Then, we prepared protein samples using the dilution method outlined above in the presence of 1 mM calcium, added EDTA (5mM) to convert D_{sat} to D^*_{apo}, and injected the samples on the SEC column. The protein stocks were at final pH values of 5.0, 5.5, 6.0, 6.5, 7.0 and 7.4.

To determine if the concentration of NaCl would impact the formation of D_{sat}, the previous experiment was performed in buffers with 60 mM, 140 mM, 500 mM, 750 mM, and 1 M NaCl at pH 7.4. The 60 mM NaCl sample was prepared by diluting the protein stock into 10 mM HEPES, pH 7.4. Samples with greater than 140 mM NaCl were prepared by adding concentrated NaCl solutions to the protein stock. Samples at each NaCl concentration were then brought to 1 mM calcium concentration and incubated for 5 min followed by addition of 5 mM EDTA and then injection on the SEC column.

Prediction of pK_a Values

To estimate the pK_a of titratable residues, we used PROPKA (3.1). It uses a five-stage empirical computing algorithm that accounts for the effects of hydrogen bonding, charge-charge interactions, and desolvation from structural data resulting in predicted pK_a values with an overall RMSD of 0.79 pH units from experimental studies [54, 66, 69, 70]. PROPKA predicted the charge of NCAD12 as -8.8 at pH 7.0. pK_a values were predicted for all ionizable residues in NCAD12 with and without the calcium ions present in the 2QVI PDB structure file [102, 103]. The 2QVI structure with calcium ions removed was not further minimized. According to PROPKA 3.1, the pI of NCAD12 is pH 4.3

Distances between residues in 2QVI crystal structure were determined with Swiss-Pdb Viewer [104-106]. Distances mentioned were from the terminal carbon of each residue's side chain to illustrate distance between charged portions of each side chain, e.g. carboxyl group of D27 to carboxyl group of E89.

RESULTS

Thermal Unfolding Studies

Thermal unfolding studies were performed to observe the impact of pH and calcium on the stability of NCAD12. The CD signal was monitored as a function of temperature. Two distinct transitions were observed with the signal becoming increasingly negative as the protein unfolded, consistent with a polyproline conformation of the unfolded state [107]. Previous work has shown that the first transition corresponds to unfolding of EC2 and the second transition to unfolding of EC1 [12]. In the absence of calcium, NCAD12 was soluble and monomeric (M_{apo}) from pH 7.4 to 6.0. NCAD12 precipitated during denaturation experiments at pH values approaching its pI, so we were unable to obtain estimates of stability at pH values below 6.0 in the apo state and below 6.5 in the calcium-saturated state (M_{sat}). For this same reason, we were unable to further study the impact of pH on EC1. As expected, the stability of NCAD12 increased in the presence of calcium.

Thermal-denaturation profiles for EC2 as a function of pH and calcium are shown in Figure 1. In the apo-state, the apparent stability of the protein increased as pH decreased. Data were fit to the Gibbs-Helmholtz equation with adjustable baseline parameters. The values resolved for T_m increased significantly as the pH decreased while the values resolved for ΔH_m decreased slightly leading to a net increase in calculated values for ΔG° at 37 ˚C (Table 1). In the presence of calcium, the thermal-denaturation profiles were indistinguishable over the accessible pH range. Identical values resolved for T_m, ΔH_m, and calculated values for $\Delta G°$ at 37 °C, indicating that the binding of calcium masks the effect of decreased pH that was observed in the apo state.

Calcium Titrations

The pH dependence of calcium-binding affinity of NCAD12 was assessed via calcium titrations monitored by CD spectroscopy. Figure 2 shows the CD signal as a function of calcium concentration at each pH. The data at each pH were normalized to correct for the pH dependence of the magnitude of the CD signal. Data are offset for clarity. The CD signal increased (less negative) with the addition of calcium at all pH values consistent with a calcium-induced increase in structure. Since the range of the CD signal over the course of the titration was low at selected wavelengths ($\Delta\Delta\varepsilon$ 2.3 ± 0.3 mdeg) for samples at pH 6.0 and 5.5, the signal to noise ratio was poor. Studies were also attempted at pH 5.0; however, protein precipitated during the titration. NCAD12 was >85 % saturated at 1 mM Ca^{2+} at all pHs.

Based on the randomness and span of residuals, data fitted well to a binding model of equal and independent sites indicating that there was no observed cooperativity in calcium binding from pH 7.4 to 5.5. There was a small, yet systematic, decrease in calcium-binding affinity as pH decreased from 7.4 to 6.0 with a significant decrease in affinity as the pH was decreased further to 5.5. This pH-dependent difference is reflected in resolved values for $\Delta G°$ in Table 2 ($\Delta\Delta G°_{7.4\text{-}6.0}$ = 0.6 kcal/mol; $\Delta\Delta G°_{6.0\text{-}5.5}$ = 0.6 kcal/mol)

Disassembly/Assembly Studies

Analytical size-exclusion chromatography (SEC) was performed to monitor the level of formation of calcium-saturated, adhesive dimer (D_{sat}) as a function of pH. To assess the level of D_{sat}, we first investigated the effect of pH on the disassembly of D^*_{apo}. The dimer eluted at ~ 11.7 mL and the monomer at ~ 12.8 mL. Previous studies of this system found that these retention volumes correspond to the calculated radius of gyration based on the crystal structures of the monomeric and strand-crossover dimer structures for classical cadherins [97]. Figure 3A shows size-exclusion chromatograms of the disassembly of D^*_{apo} as a function of pH. As pH

decreases over a range from pH 7.4 to 5.0, there is no change in the percentage of dimer (χ_D) in the sample, indicating that D^*_{apo} remained kinetically trapped. To determine if the disassembly of D^*_{apo} at low pH was time dependent, protein stock at pH 7.4 was diluted to low pH and incubated for 1 and for 5 hours before chromatographic analysis. The level of D^*_{apo} in those experiments did not change over the 5 hour time period ($\chi_D = 51 \pm 1$ %; data not shown). It was determined that a decrease in pH did not disassemble D^*_{apo}.

We monitored the level of D_{sat} by adjusting the sample to the desired pH, adding calcium to form D_{sat}, then EDTA to convert D_{sat} to D^*_{apo} for quantification via analytical SEC. This chromatographic experiment provides a 'snapshot' of the level of D_{sat} at a particular pH and concentration. Unexpectedly, with a decrease in pH, we observed an increasing trend in the fraction saturated dimer (χ_D) from 49% at pH 7.4 to 53% at pH 6.0. In this chromatographic experiment we were able to broaden our pH window to 5.0 without protein precipitation and found that χ_D continued to increase to 65% at pH 5.0. Representative size exclusion chromatograms are shown in Figure 3B, and illustrate the level of D_{sat} in solution as a function of pH. Contrary to our expectations, the level of D_{sat} systematically increased with a change in pH from 7.4 to 5.0. These results imply that the dimerization of NCAD12 increases with a decrease in pH due to protonation of acidic or histidine residues.

The increase of dimer to monomer ratio as a function of pH led us to study the effect of salt concentration on dimerization. Again, we used the level of D^*_{apo} in calcium- depleted samples to monitor the level of D_{sat} in 1 mM calcium as a function of the NaCl concentration. Dimer formation was found to increase with an increase in NaCl concentration (Figure 3C). Dissociation constants and fraction saturated dimer percentages were calculated at all pH values and salt concentrations (Table 3). Retention volume of the larger species (dimer peak) at low pH

matches the predicted radius of gyration of the dimer, and it is well within the working range of molecular weights capable of being discerned by the SEC column.

Prediction of pK_a values in NCAD12

NCAD12 is an acidic protein with 26 acidic residues and 19 basic residues, including 3 histidines. Given the canonical pK_a value for histidine, we expected that His 75, 79, and 110 would be titrated and positively charged on average in the pH range explored in our experiments. These residues are not directly associated with the calcium-binding sites, however; His 79 is located near (~10 Å) the strand-swapped interface in EC1. The three histidine residues have predicted pK_a values ranging from 5.7 to 6.3, regardless of the presence of calcium ions (Table 4).

The 17 aspartate and 9 glutamate residues in NCAD12 (221 residues) may also be protonated if their pK_a values are shifted toward the basic range, a phenomenon that is well documented for acidic residues in active sites [108] or buried in the interior of proteins [109]. Since the calcium-binding residues are in the interfacial region between adjacent modular domains, we might expect their pK_a values to be significantly shifted toward the basic range in the apo state. For this reason, we suspected all ionizable calcium binding residues [9] listed in Table 4 could have pK_a values significantly more basic than the canonical values indicating that they may impact the pH dependence of stability of NCAD12.

The results from PROPKA 3.1 computations of pK_as for all residues of interest in the presence and absence of calcium ions are shown in Table 4. We found pK_a values of calcium-binding residues were shifted toward the basic range by ~ 2 pK_a units when calcium was removed from the 2QVI structure. This effect on calculated pK_a is expected due to the density of acidic residues in the interdomain calcium-binding pocket. Four calcium-binding residues show

predicted pK_a values in the range explored in these experiments: E11, E69, D134, and D136. Residues that do not directly chelate calcium showed no shift in pK_a values when the calcium ions were removed with an average pK_a of 3.7 ± 0.8, a value close to the canonical values for free amino acids. The exception is E119, with a predicted pK_a of 5.9.

DISCUSSION

N-cadherin, a member of the classical cadherin family, is an acidic protein that requires calcium for its function as a primary cell-cell adhesion molecule in adherens junctions. It plays pivotal roles in tissue development [23, 110], cancer [26, 81] and neurological synapses [5, 111]. Due to its prominent physiological role, the structure-function relationship of N-cadherin has been of interest recently. In particular, our laboratory is interested in the effect of microenviroment on the adhesive properties of N-cadherin. The studies reported herein assess the effect of acidification on N-cadherin function. Since we expected that protonation of calcium-binding residues would decrease calcium-binding affinity, and calcium binding is required for dimerization, dimerization affinity would also decrease. Surprisingly, a decrease in pH promoted dimerization. In the following discussion, we consider pH dependent stability, calcium-binding affinity, and dimerization.

At pH 7.0, NCAD12 has a net charge of -8.8 in the native state (PROPKA 3.1), consistent with a significant impact of electrostatic repulsion in protein stability. Since a decrease in pH will lead to a net decrease in negative charge, we hypothesized that a decrease in pH should increase the stability of M_{apo}. This is what we observed in thermal denaturation studies. There is ample evidence that EC2 is destabilized by electrostatic repulsion. Previous studies from our laboratory on the stability of isolated EC2 modules, from both E-cadherin [112]

and N-cadherin [113], demonstrated that EC2 is destabilized by flanking acidic linker segments. Furthermore, this destabilization by the adjacent linker segments could be overcome by addition of NaCl. Taken together, our studies indicate that the EC2 domain is destabilized by electrostatic repulsion and can be stabilized by addition of NaCl or reduced pH.

Protonation leads to a decrease in overall negative charge due to an increase in positive charge on His residues and a decrease in negative charge of acidic residues in N-cadherin. The observed increase in stability in EC2 shown in the thermal-unfolding studies could be due to a combination of histidine and acidic residue protonation. Considering the pH window that is accessible in thermal unfolding studies (7.4-6.0), PROPKA 3.1 predicts that two residues in EC2 are protonated; H110, with an estimated pK_a of 6.3, and E119, with an estimated pK_a of 5.9 (Table 3). Given the high charge density in the calcium-binding pocket, protonation of calcium-binding residues will also support a net decrease in electrostatic repulsion.

We observed an increase in stabilization of NCAD12 as pH decreased. Thermodynamic parameters in Table 1 provide insight into the increased stabilization of EC2 as a function of pH. Based on earlier studies of isolated EC2 of E- [112] and N-cadherin [113], we expected to see an increase in T_m and a concomitant increase in the enthalpy change ($\Delta\Delta H_m$) at T_m, as net charge was reduced. However, while T_m increased in these pH-dependent studies, enthalpy decreased, albeit slightly ($\Delta\Delta H_m$ of 7 kcal/mol). Bechtel et al state that enthalpy of protonation is not a function of pH in protein stability [114]. The linear relationship between ΔH_m and T_m allows prediction of ΔC_p, yielding a ΔC_p for protonation close to 0 kcal/ (mol K). If we consider the increase in T_m, assuming ΔH_m to be constant, it would imply some decrease in entropy at T_m ($T_m * \Delta S_m = \Delta H_m$; when ΔH_m is constant). This result indicates either that decreasing the pH produces a decrease in conformational entropy, an increased exposure of hydrophobic surface

area, or a combination of both [115]. Enthalpy changes for single protonation events of Asp and Glu residues are relatively small compared to those for protein folding (ΔH_p of 0.5 to 1.5 kcal/mol) [116], possibly leading to the small, observed change in the enthalpy of unfolding as a function of pH.

We hypothesized that protonation of acidic residues in the calcium-binding pocket should lead to an overall decrease in the calcium-binding affinity. As predicted, we found that a decrease in pH did decrease calcium-binding affinity; higher calcium levels are required to populate calcium-binding sites at lower pH values. However, the magnitude of this decrease was only 0.6 kcal/mol over a 1.5 pH unit range (7.4-6.0). Additional calcium titrations at pH 5.5 showed the same reduction of 0.6 kcal/mol over a smaller pH unit range (6.0-5.5), indicating that the protonation of key acidic residues does decrease the calcium binding affinity in a pH range closer to the canonical value for protonation of acidic residues.

Previous studies on calcium binding have demonstrated the significance of D136, D134, and D103 in determining NCAD12 calcium-binding affinity. D134 is required for calcium binding at site 3, and binding at site 3 is required for calcium binding at sites 1 and 2 [98]. D136, a bidentate chelator of calcium at sites 2 and 3, is critical for ligation of both sites. The protonation of D136 or D134, or both, would increase competition between protons and calcium ions at sites 2 and 3, thus significantly decreasing overall binding affinity [98]. Based on the PROPKA 3.1, estimates of pK_a values for D134 and D136 implicated the protonation of these two residues as a possible cause for the decrease in calcium-binding affinity at lower pH values.

Our third hypothesis was that the reduction in affinity for calcium will lead to a decreased level of dimerization. Contrary to our expectations, an increase in dimer affinity at the pH values where we observed a decrease in calcium-binding affinity was observed. Salt-dependent

studies were performed to confirm that this observation could be explained by an electrostatic affect. The salt-dependent results support the argument that screening of surface charges promotes interaction between protomers, resulting in increased dimer formation. Sivasankar and Rakshit suggested that there is an, as yet uncharacterized, intermediate dimeric structure in the transition between X-dimer and strand-swapped dimer structures [117]. This proposed intermediate must bury the strand-swapped interfaces of two protomers since the spectral signal of W2 indicates that it is not exposed to solvent as it undocks and crosses over to dock in a partner protomer in the formation of the strand-swapped dimer. This intermediate implies very close contact between two protomers as the strand-swapped dimer forms. These results imply that charged residues located at the contact surface between protomers at the strand-swapped interface are responsible in tuning dimerization affinity as a function of pH.

Baumgartner et al recently demonstrated the adhesive properties of N-cadherin are pH dependent in single molecule and cellular interaction studies [31]. They reported a maximal binding activity of N-cadherin at pH 7.4 that decreased significantly over a very narrow pH range to a minimum binding activity at pH 7.0, an opposite trend to the data reported here. While our current report and Baumgartner et al both study N-cadherin, there are considerable differences in these two studies, including the methods used and the protein constructs studied. Our studies are focused on a minimal functional unit for dimerization that includes only the first two extracellular domains (EC1 and EC2), while Baumgartner et al studied a 5-domain construct. By considering our studies together, we would conclude that the effect at pH 7.0 reported by Baumgartner et al must be due to protonation events in EC3-EC5 and impose a dominant negative effect over the pH-dependent change in chemistry in EC1 and EC2 reported here. In support, Ozawa et al highlighted signal transduction through the EC-region of Type I

cadherin, and showed that a mutation in the calcium-binding sites between EC2 and EC3 causes a loss of adhesion [89].

In conclusion, within the pH range (7.4 to 5.0) NCAD12 show a pH-dependent decrease in calcium-binding affinity and increase in dimerization affinity. The change in dimerization affinity is consistent with electrostatic repulsion playing a role in moderating the affinity of dimerization. This observation begs the question of whether electrostatic interactions are definitive contributors to the tuning of the relative affinities of N-, E- and P-cadherin at the strand-crossover or X-dimer interfaces, thereby playing a role in the equilibria and kinetics of adhesion by classical cadherins.

CHAPTER III

The purpose of this chapter is to discuss aspects of the studies presented in Chapter II that were not adequately discussed in the context of the published work. The use of the two domain construct and analysis of data will be further discussed. In addition, an extended interpretation of the results will be discussed that highlights differences in E- and N-cadherin that may lead to differences in dimerization affinity.

THE TWO-DOMAIN CONSTRUCT

All studies reported in this thesis used a truncated construct containing only the first two extracellular domains of N-cadherin. NCAD12, the minimal functional unit of dimerization, is a well characterized construct [9, 67, 68]. Use of NCAD12 reduces non-specific aggregations that can occur with the five-domain construct. Using a minimal construct also lets us focus on specific residues possibly responsible for the electrostatic tuning mechanism we see. We acknowledge that differences between the NCAD12 construct expressed in E. coli cells used here and the five domain construct used in cell-based systems are potentially profound, specifically in the pH studies performed by Baumgartner et. al. It is easy to lose perspective of the five-domain physiological construct when interpreting results gathered using the abbreviated two-domain construct. NCAD12 expressed in E.coli lacks post-translational modifications and significant glycosylations that could impact pH-dependent studies [118, 119]. There is also the question concerning the physiological relevance of D*apo. We do not know if this construct occurs in vivo, but it is useful in the analytical assays implemented for dimerization studies. These

differences should be taken into account when interpreting these results and applying conclusions to physiological relevancies.

ANALYSIS OF DATA

Thermal Denaturation

The increase in stability consistent with a decrease in pH was expected. The protonation of acidic or histidine residues would decrease the net charge of an already acidic protein. The observed increase in stability could be the result of a loss of electrostatic repulsion stemming from the decrease in overall net charge of NCAD12. It would be interesting to see the effect on stability of a thermal denaturation at pH 5.5 considering the observed decrease in calcium-binding affinity at this pH. It is at pH 5.5 that we see a profound change in dimerization affinity as well. However, this was not determined due to protein precipitation. We would expect the T_m to increase again, perhaps to a greater extent than the pH 6.5-6.0 transition.

It is known that EC2 unfolds before EC1 from previous work [12]. With two distinct transitions, we can truncate the data to resolve thermodynamic values for EC2 and EC1 separately. As pH decreased, protein precipitated at higher temperatures causing a dramatic loss of signal during the EC1 unfolding transition. Previous studies show that the stability of EC2 was affected by L1 and L2, but not by EC1 [113]. This only allowed data to be resolved from EC2, therefore, all residues with estimated pKa values in the experimental range in L1-EC2-L2 must be considered. For this reason, E119, with a predicted pKa of 5.9, should be examined further. E119 is the only other non-calcium-binding residue in EC2 with an estimated pKa in our experimental range. E119 is located on the bottom of EC2 by a cluster of negatively charged residues at the AB loop within 5.7 Å of the linker 2 residue (D215) and 6.3 Å of two other acidic

residues in the EF loop (D179 and E181). Repulsion between these components would lead to an increase in energy of the domain. We would predict that the protonation of E119 would decrease the net charge and increase stability to EC2. There was no increase in stability in the calcium-bound state, presumably due to a more stable, rigid structure induced by calcium binding. This implies that calcium binds with sufficient affinity to dramatically out-compete hydrogen ions for the binding sites. To further these studies, protein denaturing studies in the presence of urea as a function of pH should be performed. Perhaps stability at lower pH values can be resolved.

Calcium-binding Affinity

The effect of pH on NCAD12 calcium-binding affinity was expected as well. A gradual decrease in calcium-binding affinity until pH 6.0 followed by a sizeable decrease at the pH 6.0-5.5 transition points to the protonation of acidic residue(s), notably calcium-binding residues. Calcium titrations were unable to be performed at pH 5.0; however, we would expect a further decrease in calcium-binding affinity. It is likely that the competitive binding between calcium and hydrogen ions at the calcium-binding sites accounts for the loss in binding affinity. It is also possible that protonation of acidic and histidine residues results in a structural change that is not conducive to calcium binding. From the results of PROPKA 3.1, we would expect the protonation of D134 and/or D136 to be responsible for the decrease in calcium-binding affinity. As stated earlier, the prediction of pKa values of residues with bound ligands is difficult despite PROPKA 3.1 being designed for such instances. For this reason, it is difficult to assign a specific residue as a main contributor to the decrease in calcium-binding affinity as a function of pH. Mutations of calcium-binding residues will not work for such studies since they will result in a decrease or loss of calcium binding all together [89, 98]. Therefore, alternate studies must be

designed for the elucidation of the pH-dependency of calcium binding on NCAD12 such as NMR [120].

Dimerization Affinity

We did not expect to see an increase in dimerization affinity coincident with a drop in pH. It was expected that the decrease in calcium-binding affinity, albeit slight, would hinder dimer formation. We believe the observed increase in dimerization is a result of the electrostatic surface of NCAD12 becoming less negatively charged. Salt-dependent studies reinforced this idea by screening charged residues, or in the pH-dependent studies' case, protonation of charged residues. Protonation of acidic residues at sites around either the X-dimer interface or SS-dimer interface, both in EC1, would reduce electrostatic repulsion between two monomers. If we consider only EC1, the possible contributors are quite limited. Through review of the strand-swapped structure of the first two domains (2QVI), we propose that D1, E20, D27, D29, and D93 are potential contributors to the interaction between protomers at the strand-swapped interface. D1, D27, and D29 are all located on the surface and within ~9 Å from the dimer interface (designated as centered of E89). E20 and D93 are located on the "strand-swapped" face of EC1, or the side of a NCAD12 protomer that faces the partner NCAD12 protomer during dimerization. All of these residues have pK_a values between 5-3. Perhaps one or more of these residues have actual pKa values closer to 5.5 where we see a dramatic shift in dimerization affinity. It is also possible that the pKa values of these residues shift when the ss-dimer forms, or for the ss-dimer to form, they must shift. Presumably, these residues are no longer exposed to solvent in the ss-dimer conformation which would result in some pKa shift toward the basic range.

Furthermore, we acknowledge that the protonation of His residues could also increase electrostatic attraction between protomers, leading to an increase in dimerization. Of course, in the case of histidine, protonation would result in a positive charge, not the loss of a negative charge. Considering that NCAD12 is an acidic protein, added positive charges would decrease the net negative charge. The three His residues have predicted pKa values in our experimental range and, presumably, are protonated. Histidine residues have been known as pH "sensors", and mutations of these residues could point to one or more being critical in the tuning of NCAD12 dimerization affinity. In particular, H79, which is located near the strand-swapped dimer interface, could be a key residue in tuning dimerization affinity. The reduction of a net negative charge at the dimer interface and "strand-swapped" face of NCAD12 would result in decreased electrostatic repulsion between protomers possibly leading to increased dimerization affinity.

pKa Empirical Computation

Assigning specific residues that account for the changes in stability, calcium-binding affinity, and dimerization affinity is difficult without the use of a computational method of predicted pKa values. Ideally, protein NMR would be implemented to experimentally determine pKa values for ionizable residues; however, the size and charge of NCAD12 brings challenges. Given the scope of the current study, it was decided to use the empirical program, PROPKA 3.1 to estimate pKa values. The 2QVI structure contains the three calcium ions bound to NCAD12 in its monomeric form. The presence of calcium ions can hinder proper pKa calculation due to the empirical nature of PROPKA 3.1. Bound ions can influence the pKa values of surrounding residues. These shifts in pKa values can be difficult for an empirical program, such as PROPKA, to detect. To account for this, we also implemented a second computational program

to compare estimated pKa values to PROPKA. H^{++} uses a continuum electrostatic model to solve the Poisson-Boltzmann equation[121]. Specifically, we wanted to look for differences in estimated pKa values of the calcium-binding residues. Resulting estimated pKa values were drastically shifted to the basic range compared to PROPKA 3.1. Most all titratable residues were shown to have pKa values above 11 despite solvent exposure. In the case of calcium-binding residues, D103 has an estimated pKa at 7.6, all others having pKa values above 11. The large pKa values of these residues were confusing, in that, it would be highly unlikely that all acidic residues would have pKa values above 11, even if all were buried. Considering we don't see a shift in calcium binding until around pH 6.0, it was determined that H^{++} was not ideal for NCAD12.

COMPARISON OF E- AND N-CADHERIN

A comparison of sequences of E-cadherin to N-cadherin provides the basis of hypotheses on the pH-dependency of the former. Sequence comparisons were performed by the program LALIGN[122] and are shown in Figure 4. Considering that ECAD12 has a lower pI and more negatively charged at physiological pH, one would predict that pH would have a larger effect than on NCAD12. Figure 5 shows the location of titratable residues in ECAD12 and NCAD12. ECAD12 has two more basic residues and eight more acidic residues than NCAD12. In EC1 alone, there are four more acidic residues. Most titratable residues are located around the calcium-binding sites and dimer interfaces in both structures. ECAD12 has an abundance of titratable residues located at the SS-dimer interface that could be responsible for tuning dimerization affinity. Figure 6 identifies all titratable residues in EC1 of ECAD12. The ratio of acidic to basic residues in the SS-dimer region could govern ECAD12's susceptibility to pH.

Specifically, we would look at residues D1, K25, R28, D29, K30, E31, K33, E56, E89, D90, and D93. These residues would, presumably, factor into an electrostatic tuning mechanism due to their proximity to the SS-dimer interface. Our NCAD12 dimerization-affinity studies show that residues in this location can effect dimerization dramatically as pH decreases. In the case of potential ECAD12 studies, we could perform the experiments done on NCAD12, including computational work.

These experiments provide a foundation for future work that can further characterized NCAD12 as a pH-dependent protein. The ultimate goal of identifying critical amino acid residues that act as switches for the electrostatic tuning mechanism can be accomplished with single-site mutant studies. Results show that with a drop in pH, NCAD12 exhibits an increase in stability, decrease in calcium-binding affinity, and an increase in dimerization affinity. From these results we can conclude that NCAD12 is sensitive to an electrostatic tuning mechanism due to the protonation of acidic or histidine residues.

LIST OF REFERENCES

REFERENCES

1. Nollet, F., P. Kools, and F. Van Roy, *Phylogenetic analysis of the cadherin superfamily allows identification of six major subfamilies besides several solitary members.* Journal of molecular biology, 2000. **299**(3): p. 551-572.
2. Ranscht, B., *Cadherins and catenins: interactions and functions in embryonic development.* Current opinion in cell biology, 1994. **6**(5): p. 740-746.
3. Alattia, J.R., H. Kurokawa, and M. Ikura, *Structural view of cadherin-mediated cell-cell adhesion.* Cell Mol Life Sci, 1999. **55**(3): p. 359-67.
4. Gumbiner, B.M., *Cell adhesion: the molecular basis of tissue architecture and morphogenesis.* Cell, 1996. **84**(3): p. 345-357.
5. Takeichi, M., *Cadherin cell adhesion receptors as a morphogenetic regulator.* Science, 1991. **251**(5000): p. 1451-5.
6. Tepass, U., et al., *Cadherins in embryonic and neural morphogenesis.* Nat Rev Mol Cell Biol, 2000. **1**(2): p. 91-100.
7. Larue, L., et al., *E-cadherin null mutant embryos fail to form a trophectoderm epithelium.* Proceedings of the National Academy of Sciences, 1994. **91**(17): p. 8263-8267.
8. Shapiro, L., et al., *Considerations on the folding topology and evolutionary origin of cadherin domains.* Proceedings of the National Academy of Sciences, 1995. **92**(15): p. 6793-6797.
9. Tamura, K., et al., *Structure-function analysis of cell adhesion by neural (N-) cadherin.* Neuron, 1998. **20**(6): p. 1153-63.
10. Pertz, O., et al., *A new crystal structure, Ca2+ dependence and mutational analysis reveal molecular details of E-cadherin homoassociation.* Embo J, 1999. **18**(7): p. 1738-47.
11. Perret, E., et al., *Fast dissociation kinetics between individual E-cadherin fragments revealed by flow chamber analysis.* Embo J, 2002. **21**(11): p. 2537-46.
12. Vunnam, N. and S. Pedigo, *Prolines in betaA-Sheet of Neural Cadherin Act as a Switch To Control the Dynamics of the Equilibrium between Monomer and Dimer.* Biochemistry, 2011. **50**(32): p. 6959-6965.
13. Vendome, J., et al., *Molecular design principles underlying beta-strand swapping in the adhesive dimerization of cadherins.* Nat Struct Mol Biol, 2011. **18**(6): p. 693-700.
14. Pokutta, S., et al., *Conformational changes of the recombinant extracellular domain of E-cadherin upon calcium binding.* Eur J Biochem, 1994. **223**(3): p. 1019-26.
15. Koch, A.W., et al., *Calcium binding and homoassociation of E-cadherin domains.* Biochemistry, 1997. **36**(25): p. 7697-705.
16. Sivasankar, S., et al., *Direct molecular force measurements of multiple adhesive interactions between cadherin ectodomains.* Proc Natl Acad Sci U S A, 1999. **96**(21): p. 11820-4.

17. Shan, W.-S., et al., *Functional cis-heterodimers of N-and R-cadherins.* The Journal of cell biology, 2000. **148**(3): p. 579-590.
18. Ahrens, T., et al., *Analysis of heterophilic and homophilic interactions of cadherins using the c-Jun/c-Fos dimerization domains.* Journal of Biological Chemistry, 2002. **277**(22): p. 19455-19460.
19. Murphy-Erdosh, C., et al., *The cadherin-binding specificities of B-cadherin and LCAM.* The Journal of cell biology, 1995. **129**(5): p. 1379-1390.
20. Shapiro, L., et al., *Structural basis of cell-cell adhesion by cadherins [see comments]*. Nature, 1995. **374**(6520): p. 327-37.
21. Boggon, T.J., et al., *C-cadherin ectodomain structure and implications for cell adhesion mechanisms.* Science, 2002. **296**(5571): p. 1308-13.
22. Blaschuk, O.W., et al., *Identification of a cadherin cell adhesion recognition sequence.* Developmental biology, 1990. **139**(1): p. 227-229.
23. Hatta, K. and M. Takeichi, *Expression of N-cadherin adhesion molecules associated with early morphogenetic events in chick development.* 1986.
24. Hatta, K., T. Okada, and M. Takeichi, *A monoclonal antibody disrupting calcium-dependent cell-cell adhesion of brain tissues: possible role of its target antigen in animal pattern formation.* Proceedings of the National Academy of Sciences, 1985. **82**(9): p. 2789-2793.
25. Blaschuk, O.W. and T.M. Rowlands, *Cadherins as modulators of angiogenesis and the structural integrity of blood vessels.* Cancer and Metastasis Reviews, 2000. **19**(1-2): p. 1-5.
26. Hazan, R.B., et al., *Exogenous expression of N-cadherin in breast cancer cells induces cell migration, invasion, and metastasis.* The Journal of cell biology, 2000. **148**(4): p. 779-790.
27. Benson, D.L. and H. Tanaka, *N-cadherin redistribution during synaptogenesis in hippocampal neurons.* J Neurosci, 1998. **18**(17): p. 6892-904.
28. Tan, Z.-J., et al., *N-cadherin-dependent neuron–neuron interaction is required for the maintenance of activity-induced dendrite growth.* Proceedings of the National Academy of Sciences, 2010. **107**(21): p. 9873-9878.
29. Bronner-Fraser, M., J.J. Wolf, and B.A. Murray, *Effects of antibodies against N-cadherin and N-CAM on the cranial neural crest and neural tube.* Developmental biology, 1992. **153**(2): p. 291-301.
30. Bozdagi, O., et al., *Increasing numbers of synaptic puncta during late-phase LTP: N-cadherin is synthesized, recruited to synaptic sites, and required for potentiation.* Neuron, 2000. **28**(1): p. 245-59.
31. Baumgartner, W., et al., *Different pH-dependencies of the two synaptic adhesion molecules N-cadherin and cadherin-11 and the possible functional implication for long-term potentiation.* Synapse, 2013. **67**(10): p. 705-715.
32. Siitonen, S.M., et al., *Reduced E-cadherin expression is associated with invasiveness and unfavorable prognosis in breast cancer.* American journal of clinical pathology, 1996. **105**(4): p. 394-402.
33. Nieman, M.T., et al., *N-cadherin promotes motility in human breast cancer cells regardless of their E-cadherin expression.* J Cell Biol, 1999. **147**(3): p. 631-44.
34. Paul, R., et al., *The cadherin cell-cell adhesion pathway in prostate cancer progression.* British journal of urology, 1997. **79**: p. 37-43.

35. Wheelock, M.J., et al., *Cadherin switching.* Journal of cell science, 2008. **121**(6): p. 727-735.
36. Birchmeier, C., W. Birchmeier, and B. Brand-Saberi, *Epithelial-mesenchymal transitions in cancer progression.* Cells Tissues Organs, 1996. **156**(3): p. 217-226.
37. Nieman, M.T., et al., *N-cadherin promotes motility in human breast cancer cells regardless of their E-cadherin expression.* The Journal of cell biology, 1999. **147**(3): p. 631-644.
38. Cavallaro, U. and G. Christofori, *Cell adhesion and signalling by cadherins and Ig-CAMs in cancer.* Nature Reviews Cancer, 2004. **4**(2): p. 118-132.
39. Suyama, K., et al., *A signaling pathway leading to metastasis is controlled by N-cadherin and the FGF receptor.* Cancer cell, 2002. **2**(4): p. 301-314.
40. Ramos-DeSimone, N., et al., *Activation of matrix metalloproteinase-9 (MMP-9) via a converging plasmin/stromelysin-1 cascade enhances tumor cell invasion.* Journal of Biological Chemistry, 1999. **274**(19): p. 13066-13076.
41. Itoh, T., et al., *Experimental metastasis is suppressed in MMP-9-deficient mice.* Clinical & experimental metastasis, 1999. **17**(2): p. 177-181.
42. Webb, B.A., et al., *Dysregulated pH: a perfect storm for cancer progression.* Nature Reviews Cancer, 2011. **11**(9): p. 671-677.
43. Gerweck, L.E. and K. Seetharaman, *Cellular pH gradient in tumor versus normal tissue: potential exploitation for the treatment of cancer.* Cancer research, 1996. **56**(6): p. 1194-1198.
44. Michaelson, D.M. and I. Angel, *Determination of ΔpH in cholinergic synaptic vesicles: its effect on storage and release of acetylcholine.* Life sciences, 1980. **27**(1): p. 39-44.
45. Miesenböck, G., D.A. De Angelis, and J.E. Rothman, *Visualizing secretion and synaptic transmission with pH-sensitive green fluorescent proteins.* Nature, 1998. **394**(6689): p. 192-195.
46. Wemmie, J.A., X.-m. Zha, and M.J. Welsh, *Acid-sensing ion channels (ASICs) and pH in synapse physiology*, in *Structural and Functional Organization of the Synapse*. 2008, Springer. p. 661-681.
47. Doster, W., et al., *Control and pH dependence of ligand binding to heme proteins.* Biochemistry, 1982. **21**(20): p. 4831-4839.
48. Tollinger, M., et al., *Site-specific contributions to the pH dependence of protein stability.* Proceedings of the National Academy of Sciences, 2003. **100**(8): p. 4545-4550.
49. Swietnicki, W., et al., *pH-dependent stability and conformation of the recombinant human prion protein PrP (90–231).* Journal of Biological Chemistry, 1997. **272**(44): p. 27517-27520.
50. Yang, A.-S. and B. Honig, *On the pH dependence of protein stability.* Journal of molecular biology, 1993. **231**(2): p. 459-474.
51. Carroll, J.A., C.F. Garon, and T.G. Schwan, *Effects of environmental pH on membrane proteins in Borrelia burgdorferi.* Infection and immunity, 1999. **67**(7): p. 3181-3187.
52. Forsyth, W.R., J.M. Antosiewicz, and A.D. Robertson, *Empirical relationships between protein structure and carboxyl pKa values in proteins.* Proteins: Structure, Function, and Bioinformatics, 2002. **48**(2): p. 388-403.
53. Li, H., A.D. Robertson, and J.H. Jensen, *The determinants of carboxyl pKa values in turkey ovomucoid third domain.* Proteins: Structure, Function, and Bioinformatics, 2004. **55**(3): p. 689-704.

54. Li, H., A.D. Robertson, and J.H. Jensen, *Very fast empirical prediction and rationalization of protein pKa values.* Proteins: Structure, Function, and Bioinformatics, 2005. **61**(4): p. 704-721.
55. Tishmack, P.A., et al., *Use of 1H NMR Spectroscopy and Computer Simulations To Analyze Histidine p K a Changes in a Protein Tyrosine Phosphatase: Experimental and Theoretical Determination of Electrostatic Properties in a Small Protein.* Biochemistry, 1997. **36**(39): p. 11984-11994.
56. Markley, J.L. and I.B. Ibanez, *Zymogen activation in serine proteinases. Proton magnetic resonance pH titration studies of the two histidines of bovine chymotrypsinogen A and chymotrypsin A. alpha.* Biochemistry, 1978. **17**(22): p. 4627-4640.
57. Rajan, S., et al., *TASK-3, a Novel Tandem Pore Domain Acid-sensitive K+ Channel AN EXTRACELLULAR HISTIDINE AS pH SENSOR.* Journal of Biological Chemistry, 2000. **275**(22): p. 16650-16657.
58. Gerchman, Y., et al., *Histidine-226 is part of the pH sensor of NhaA, a Na+/H+ antiporter in Escherichia coli.* Proceedings of the National Academy of Sciences, 1993. **90**(4): p. 1212-1216.
59. Gilson, M.K., et al., *On the calculation of electrostatic interactions in proteins.* Journal of molecular biology, 1985. **184**(3): p. 503-516.
60. Kukic, P. and J.E. Nielsen, *Electrostatics in proteins and protein-ligand complexes.* Future medicinal chemistry, 2010. **2**(4): p. 647-666.
61. Honig, B. and A. Nicholls, *Classical electrostatics in biology and chemistry.* SCIENCE-NEW YORK THEN WASHINGTON-, 1995: p. 1144-1144.
62. Alexov, E., et al., *Progress in the prediction of pKa values in proteins.* Proteins: Structure, Function, and Bioinformatics, 2011. **79**(12): p. 3260-3275.
63. Barth, P., T. Alber, and P. Harbury, *Accurate, conformation-dependent predictions of solvent effects on protein ionization constants.* Proceedings of the National Academy of Sciences, 2007. **104**(12): p. 4898-4903.
64. Davies, M.N., et al., *Benchmarking pKa prediction.* BMC biochemistry, 2006. **7**(1): p. 18.
65. Marino, S.M. and V.N. Gladyshev, *Analysis and functional prediction of reactive cysteine residues.* Journal of Biological Chemistry, 2012. **287**(7): p. 4419-4425.
66. Bas, D.C., D.M. Rogers, and J.H. Jensen, *Very fast prediction and rationalization of pKa values for protein–ligand complexes.* Proteins: Structure, Function, and Bioinformatics, 2008. **73**(3): p. 765-783.
67. Nagar, B., et al., *Structural basis of calcium-induced E-cadherin rigidification and dimerization.* Nature, 1996. **380**(6572): p. 360-4.
68. Shan, W., et al., *The minimal essential unit for cadherin-mediated intercellular adhesion comprises extracellular domains 1 and 2.* J Biol Chem, 2004. **279**(53): p. 55914-23.
69. Olsson, M.H., et al., *PROPKA3: consistent treatment of internal and surface residues in empirical p K a predictions.* Journal of Chemical Theory and Computation, 2011. **7**(2): p. 525-537.
70. Søndergaard, C.R., et al., *Improved treatment of ligands and coupling effects in empirical calculation and rationalization of p K a values.* Journal of Chemical Theory and Computation, 2011. **7**(7): p. 2284-2295.
71. Gerweck, L.E. and K. Seetharaman, *Cellular pH gradient in tumor versus normal tissue: potential exploitation for the treatment of cancer.* Cancer Res, 1996. **56**(6): p. 1194-8.

72. Stuwe, L., et al., *pH dependence of melanoma cell migration: protons extruded by NHE1 dominate protons of the bulk solution.* J Physiol, 2007. **585**(Pt 2): p. 351-60.
73. Perillie, P.E., J. Nolan, and S. Finch, *Studies of the resistance to infection in diabetes mellitus: local exudative cellular response.* J Lab Clin Med, 1962. **59**(1008): p. 15.
74. Lardner, A., *The effects of extracellular pH on immune function.* Journal of leukocyte biology, 2001. **69**(4): p. 522-530.
75. Oster, J. and M. Epstein, *Acid-base aspects of ketoacidosis.* American journal of nephrology, 1984. **4**(3): p. 137-151.
76. Krishtal, O.A., et al., *Rapid extracellular pH transients related to synaptic transmission in rat hippocampal slices.* Brain Res, 1987. **436**(2): p. 352-6.
77. Yu, X. and R.C. Malenka, *Multiple functions for the cadherin/catenin complex during neuronal development.* Neuropharmacology, 2004. **47**(5): p. 779-86.
78. Fannon, A.M. and D.R. Colman, *A model for central synaptic junctional complex formation based on the differential adhesive specificities of the cadherins.* Neuron, 1996. **17**(3): p. 423-34.
79. Gravdal, K., et al., *A switch from E-cadherin to N-cadherin expression indicates epithelial to mesenchymal transition and is of strong and independent importance for the progress of prostate cancer.* Clinical Cancer Research, 2007. **13**(23): p. 7003-7011.
80. Li, G., K. Satyamoorthy, and M. Herlyn, *N-cadherin-mediated intercellular interactions promote survival and migration of melanoma cells.* Cancer research, 2001. **61**(9): p. 3819-3825.
81. Islam, S., et al., *Expression of N-cadherin by human squamous carcinoma cells induces a scattered fibroblastic phenotype with disrupted cell-cell adhesion.* The Journal of cell biology, 1996. **135**(6): p. 1643-1654.
82. Warburg, O., *On the origin of cancer cells.* Science, 1956. **123**(3191): p. 309-14.
83. Warburg, O., F. Wind, and E. Negelein, *The metabolism of tumors in the body.* The Journal of general physiology, 1927. **8**(6): p. 519-530.
84. Pokutta, S. and W.I. Weis, *Structure and mechanism of cadherins and catenins in cell-cell contacts.* Annu Rev Cell Dev Biol, 2007. **23**: p. 237-61.
85. Vleminckx, K. and R. Kemler, *Cadherins and tissue formation: integrating adhesion and signaling.* Bioessays, 1999. **21**(3): p. 211-20.
86. Haussinger, D., et al., *Proteolytic E-cadherin activation followed by solution NMR and X-ray crystallography.* Embo J, 2004. **23**(8): p. 1699-708.
87. Patel, S.D., et al., *Type II cadherin ectodomain structures: implications for classical cadherin specificity.* Cell, 2006. **124**(6): p. 1255-68.
88. Shan, W., et al., *The minimal essential unit for cadherin-mediated intercellular adhesion comprises extracellular domains 1 and 2.* Journal of Biological Chemistry, 2004. **279**(53): p. 55914-55923.
89. Ozawa, M., J. Engel, and R. Kemler, *Single amino acid substitutions in one Ca2+ binding site of uvomorulin abolish the adhesive function.* Cell, 1990. **63**(5): p. 1033-8.
90. Prakasam, A., et al., *Calcium site mutations in cadherin: impact on adhesion and evidence of cooperativity.* Biochemistry, 2006. **45**(22): p. 6930-9.
91. Creighton, T.E., *Proteins: structures and molecular properties*. 2nd ed. 1993, New York: W. H. Freeman.

92. Qin, J., G.M. Clore, and A.M. Gronenborn, *Ionization equilibria for side-chain carboxyl groups in oxidized and reduced human thioredoxin and in the complex with its target peptide from the transcription factor NFκB.* Biochemistry, 1996. **35**(1): p. 7-13.
93. Karp, D.A., et al., *High apparent dielectric constant inside a protein reflects structural reorganization coupled to the ionization of an internal Asp.* Biophysical journal, 2007. **92**(6): p. 2041-2053.
94. Karp, D.A., M.R. Stahley, and B. García-Moreno E, *Conformational consequences of ionization of Lys, Asp, and Glu buried at position 66 in staphylococcal nuclease.* Biochemistry, 2010. **49**(19): p. 4138-4146.
95. Fritz, R., K. Stiasny, and F.X. Heinz, *Identification of specific histidines as pH sensors in flavivirus membrane fusion.* The Journal of cell biology, 2008. **183**(2): p. 353-361.
96. Achilonu, I., et al., *Role of individual histidines in the pH-dependent global stability of human chloride intracellular channel 1.* Biochemistry, 2012. **51**(5): p. 995-1004.
97. Vunnam, N., et al., *Dimeric States of Neural- and Epithelial-Cadherins are Distinguished by the Rate of Disassembly.* Biochemistry, 2011. **50**(14): p. 2951-61.
98. Vunnam, N. and S. Pedigo, *Sequential binding of calcium leads to dimerization in neural cadherin.* Biochemistry, 2011. **50**(14): p. 2973-82.
99. Laemmli, U.K., *Cleavage of structural proteins during the assembly of the head of bacteriophage T4.* nature, 1970. **227**(5259): p. 680-685.
100. Edelhoch, H., *Spectroscopic determination of tryptophan and tyrosine in proteins.* Biochemistry, 1967. **6**(7): p. 1948-54.
101. Prasad, A., N.A. Housley, and S. Pedigo, *Thermodynamic stability of domain 2 of epithelial cadherin.* Biochemistry, 2004. **43**(25): p. 8055-66.
102. Berman, H.M., et al., *The protein data bank.* Nucleic acids research, 2000. **28**(1): p. 235-242.
103. Shapiro, L.S., Carroll, K.J., Honig, B., *Biophysical characterization of N-cadherin and E-cadherin homophilic and heterophilic interactions*. 2008.
104. Johansson, M.U., et al., *Defining and searching for structural motifs using DeepView/Swiss-PdbViewer.* BMC bioinformatics, 2012. **13**(1): p. 173.
105. Guex, N., M.C. Peitsch, and T. Schwede, *Automated comparative protein structure modeling with SWISS-MODEL and Swiss-PdbViewer: A historical perspective.* Electrophoresis, 2009. **30**(S1): p. S162-S173.
106. Schwede, T., et al., *SWISS-MODEL: an automated protein homology-modeling server.* Nucleic acids research, 2003. **31**(13): p. 3381-3385.
107. Greenfield, N. and G.D. Fasman, *Computed circular dichroism spectra for the evaluation of protein conformation.* Biochemistry, 1969. **8**(10): p. 4108-16.
108. Nielsen, J.E. and J.A. McCammon, *Calculating pKa values in enzyme active sites.* Protein Science, 2003. **12**(9): p. 1894-1901.
109. Meyer, T., G. Kieseritzky, and E.W. Knapp, *Electrostatic pKa computations in proteins: Role of internal cavities.* Proteins: Structure, Function, and Bioinformatics, 2011. **79**(12): p. 3320-3332.
110. Inuzuka, H., C. Redies, and M. Takeichi, *Differential expression of R-and N-cadherin in neural and mesodermal tissues during early chicken development.* Development, 1991. **113**(3): p. 959-967.
111. Takai, Y., K. Shimizu, and T. Ohtsuka, *The roles of cadherins and nectins in interneuronal synapse formation.* Curr Opin Neurobiol, 2003. **13**(5): p. 520-6.

112. Prasad, A., et al., *Effect of linker segments upon the stability of Epithelial-Cadherin Domain 2.* Proteins, 2006. **62**(1): p. 111-121.
113. Vunnam, N., et al., *Stability Studies of Extracellular Domain Two of Neural-Cadherin.* Biochim Biophys Acta, 2011. ***14***(12): p. 1841-1845.
114. Becktel, W.J. and J.A. Schellman, *Protein stability curves.* Biopolymers, 1987. **26**(11): p. 1859-77.
115. Pace, C.N., *Contribution of the hydrophobic effect to globular protein stability.* Journal of molecular biology, 1992. **226**(1): p. 29-35.
116. Kitzinger, C. and R. Hems, *Enthalpies of hydrolysis of glutamine and asparagine and of ionization of glutamic and aspartic acids.* Biochemical Journal, 1959. **71**(2): p. 395.
117. Rakshit, S., et al., *Ideal, catch, and slip bonds in cadherin adhesion.* Proceedings of the National Academy of Sciences, 2012. **109**(46): p. 18815-18820.
118. Guo, H.-B., et al., *Regulation of homotypic cell-cell adhesion by branched N-glycosylation of N-cadherin extracellular EC2 and EC3 domains.* Journal of Biological Chemistry, 2009. **284**(50): p. 34986-34997.
119. Liwosz, A., T. Lei, and M.A. Kukuruzinska, *N-glycosylation affects the molecular organization and stability of E-cadherin junctions.* Journal of Biological Chemistry, 2006. **281**(32): p. 23138-23149.
120. Schaller, W. and A.D. Robertson, *pH, ionic strength, and temperature dependences of ionization equilibria for the carboxyl groups in turkey ovomucoid third domain.* Biochemistry, 1995. **34**(14): p. 4714-23.
121. Gordon, J.C., et al., *H++: a server for estimating pKas and adding missing hydrogens to macromolecules.* Nucleic acids research, 2005. **33**(suppl 2): p. W368-W371.
122. Pearson, W., *LALIGN-find multiple matching subsegments in two sequences*. 1991.

LIST OF APPENDICIES

APPENDIX A: TABLES

Table 1. Results from Thermal Denaturation Experiments[a]

Buffer	Protein State	ΔH_m (kcal/mol)	T_m (°C)	$\Delta G^{\circ b}$ (kcal/mol)
pH 7.4	apo	74 ± 3	44.0 ± 0.1	1.6 ± 0.2
	Ca	90 ± 3	56.6 ± 0.1	4.8 ± 0.2
pH 7.0	apo	71 ± 3	44.7 ± 0.2	1.6 ± 0.1
	Ca	91 ± 5	56.3 ± 0.2	4.8 ± 0.1
pH 6.5	apo	71 ± 3	46.0 ± 0.2	1.9 ± 0.2
	Ca	94 ± 2	56.2 ± 0.1	4.9 ± 0.2
pH 6.0	apo	67 ± 2	48.5 ± 0.5	2.2 ± 0.2

[a] Gibbs Helmholtz equation where ΔC_p was fixed at 1 kcal mol^{-1} K^{-1}[97]. Reported errors were resolved from global analysis of replicate experiments.

[b] Values were calculated at 37 °C.

Table 2: Free Energies of Calcium Binding Resolved from Analysis of Calcium Titrations

pH	ΔG°[a] (kcal/mol)
7.4	-6.2 ± 0.2
7.0	-6.0 ± 0.2
6.5	-5.8 ± 0.3
6.0	-5.6 ± 0.3
5.5	-5.0 ± 0.2

[a] Values were calculated at 25 °C

Table 3. Results from Analytical SEC for the Assembly of the Calcium-Saturated Dimer

pH	K_d (μM)	χ_D (%)	ΔG° (kcal/mol)	[NaCl]	K_d (μM)	χ_D (%)	ΔG° (kcal/mol)
7.4	25 ± 3	49 ± 3	2.2 ± 0.1	60 mM	40 ± 1	39 ± 1	1.9 ± 0.1
7.0	23 ± 4	50 ± 3	2.2 ± 0.1	140 mM	31 ± 5	45 ± 4	2.0 ± 0.1
6.5	21 ± 2	52 ± 2	2.3 ± 0.1	500 mM	23 ± 2	48 ± 1	2.2 ± 0.1
6.0	20 ± 2	53 ± 3	2.3 ± 0.1	750 mM	21 ± 3	50 ± 2	2.3 ± 0.1
5.5	14 ± 1	58 ± 1	2.5 ± 0.1	1 M	13 ± 2	57 ± 2	2.6 ± 0.1
5.0	9 ± 1	65 ± 1	2.8 ± 0.1	-	-	-	-

Table 4. Results from PROPKA Predictions.

Residue	Predicted pK_a[a]	Predicted pK_a[b]	Model pK_a
D27	4.0	4.0	3.8
D29	2.5	2.5	3.8
D67[c]	1.3	2.4	3.8
D93	3.7	3.7	3.8
D103[c]	2.3	4.1	3.8
D134[c]	6.2	7.4	3.8
D136[c]	3.2	5.6	3.8
D194[c]	3.6	4.4	3.8
E11[c]	7.5	9.1	4.5
E69[c]	4.7	6.3	4.5
E89	3.3	3.3	4.5
E119	5.9	5.9	4.5
H75	6.1	6.1	6.1
H79	5.7	5.7	6.1
H110	6.3	6.3	6.1

[a] Calcium ions retained in 2QVI structure

[b] Calcium ions removed from 2QVI structure

[c] Calcium-binding residues

APPENDIX B: FIGURES

FIGURE 1:

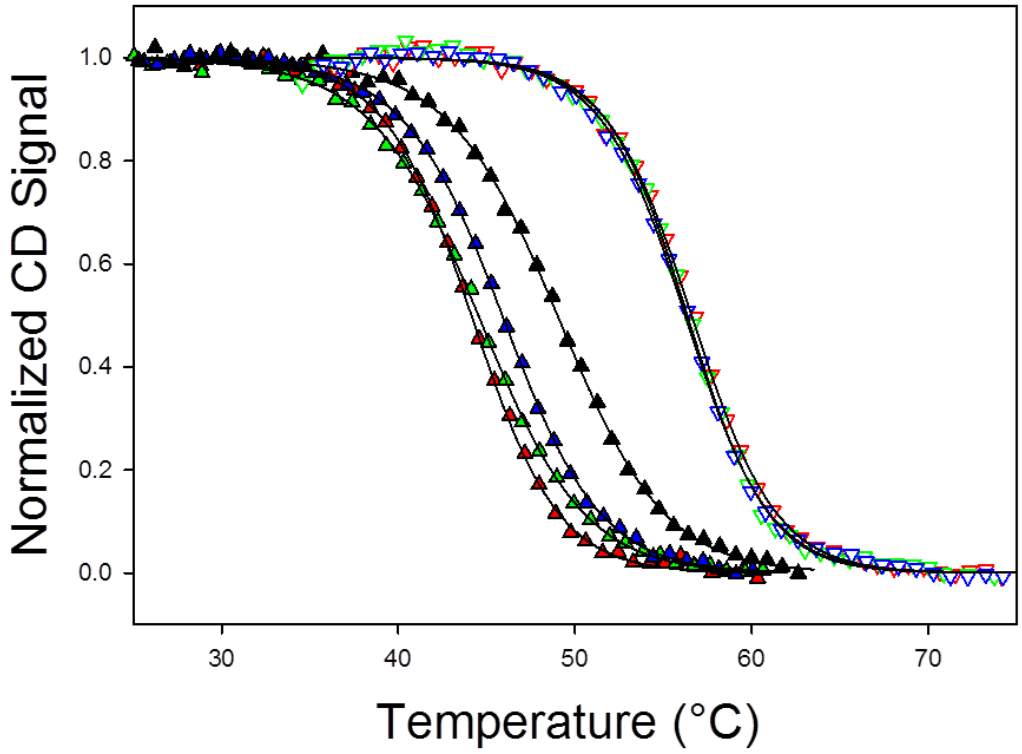

Figure 1: Thermal denaturation of NCAD12 as a function of pH and calcium. First unfolding transition of NCAD12 at pH 7.4 (red), 7.0 (green), 6.5 (blue), and 6.0 (black) are shown in the apo state (closed) and with 2.5 mM Ca^{2+} added (open). CD signal at 227 nm is reported. Solid lines are simulated based on parameters resolved from the Gibbs-Helmholtz equation. Resolved Free energy values are given in Table 1.

FIGURE 2:

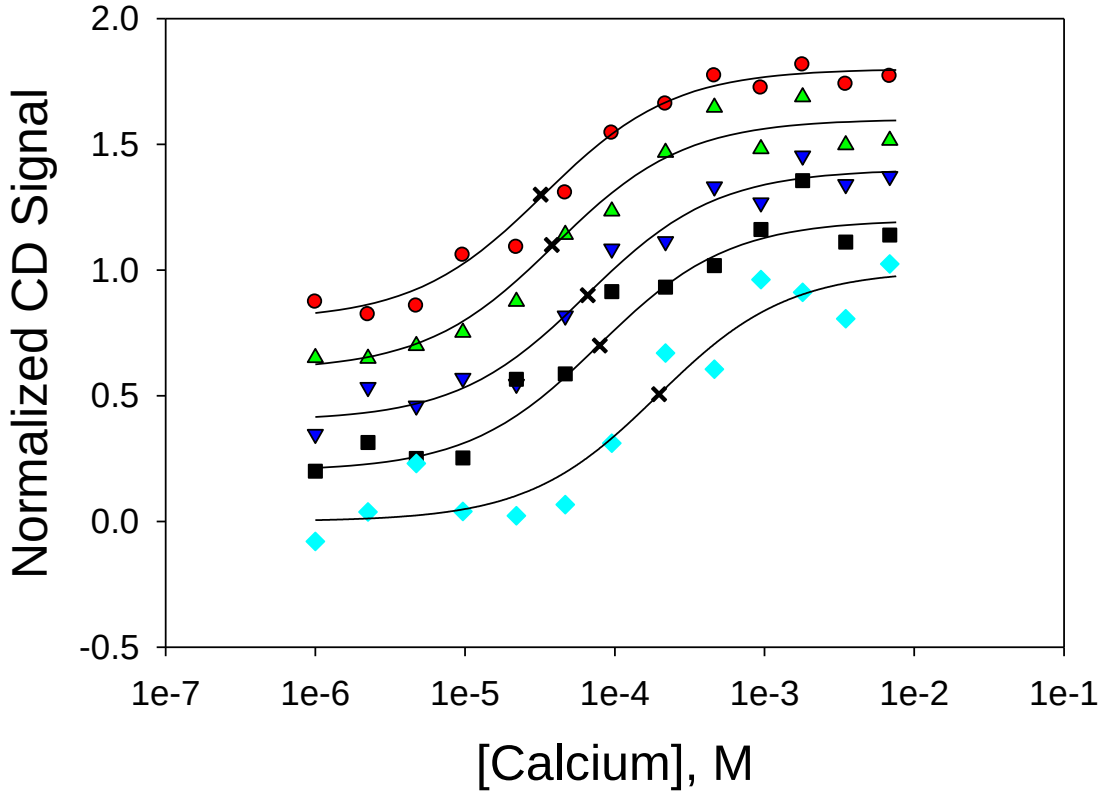

Figure 2: Calcium titrations of NCAD12 as a function of pH. NCAD12 was titrated with calcium at pH 7.4 (red), 7.0 (green), 6.5 (blue), 6.0 (black), and 5.5 (cyan); the CD signal is plotted against total calcium concentration. Solid lines are simulated based of parameters resolved from global analysis of at least two separate experiments. Data are normalized and offset for clarity. Resolved values for the change in free energy of binding are shown in Table 2.

FIGURE 3:

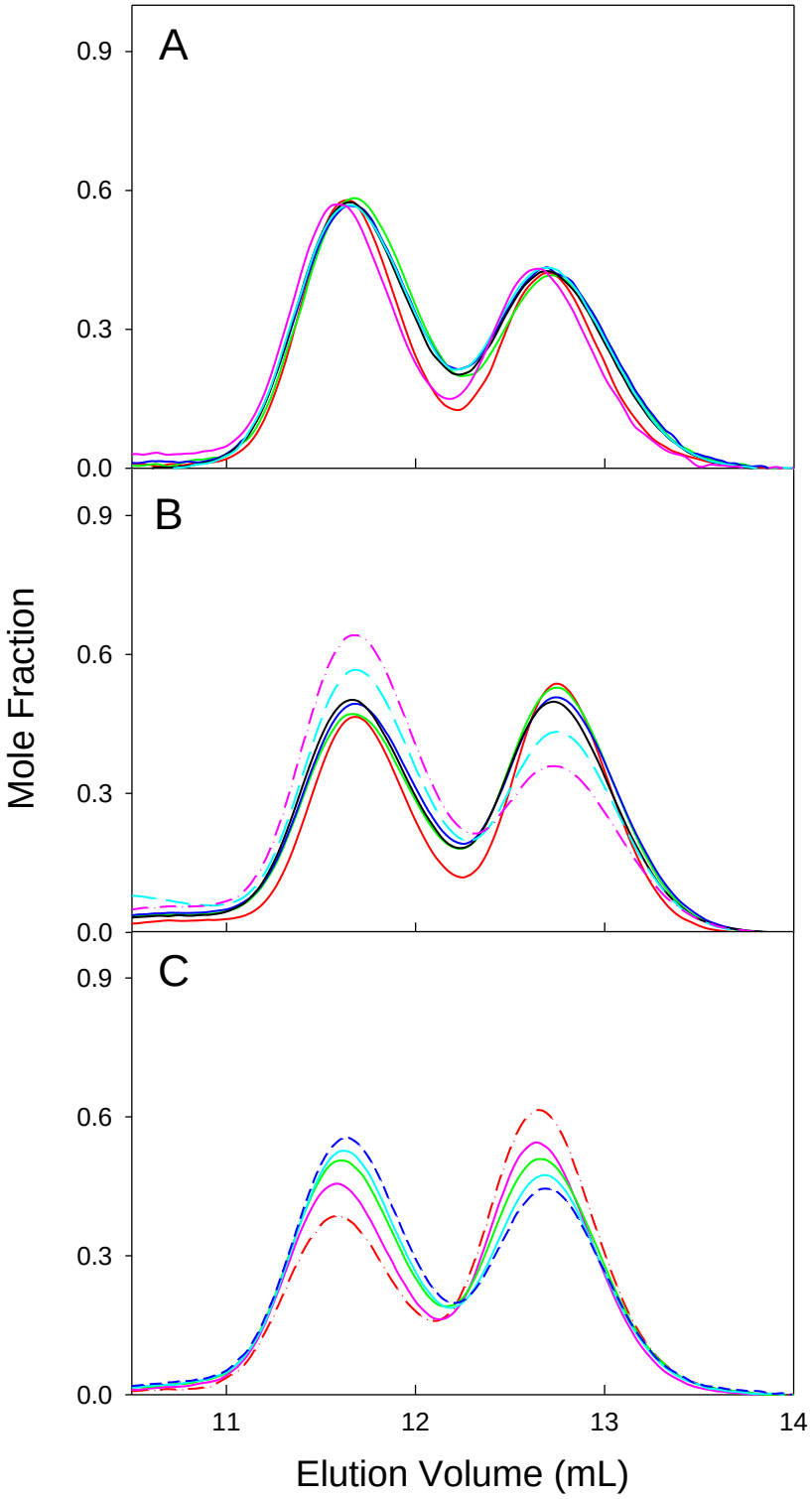

Figure 3: Analytical SEC chromatograms to assess the impact of pH on the disassembly of D^*_{apo} (A) and assembly of D_{sat} (B) at pH 7.4 (red), pH 7.0 (green), pH 6.5 (blue), pH 6.0 (black), pH 5.5 (cyan), and pH 5.0 (pink). Analytical SEC chromatograms to assess the impact of NaCl concentrations (C) at 60 mM (red-dash/dot), 140 mM (pink), 500 mM (green), 750 mM (cyan), and 1 M (blue-dash) on the assembly of D_{sat}. Y-axis was normalized to reflect dimer percentage. Resolved free energy and dissociation values for (B) and (C) are in Table 3

FIGURE 4:

```
E-  DWVIPPISCPENEKGEFPKNLVQIKSNRDKETKVFYSITGQGADKPPVGVFIIERETGWL
    :::::::. ::: .: ::.:::.:.:.:::. .. ::.:: :::.:::.:.:::.  .: :
N-  DWVIPPINLPENSRGPFPQELVRIRSDRDKNLSLRYSVTGPGADQPPTGIFIINPISGQL

E-  KVTQPLDREAIAKYILYSHAVSSNGEAVEDPMEIVITVTDQNDNRPEFTQEVFEGSVAEG
    .::.:::::: ::.. : .::::. ::. ::.:.:::.: :.:::::::: ..:.:::: ::
N-  SVTKPLDRELIARFHLRAHAVDINGNQVENPIDIVINVIDMNDNRPEFLHQVWNGSVPEG

E-  AVPGTSVMKVSATDADDDVNTYNAAIAYTIVSQDPELPHKNMFTVNRDTGVISVLTSGLD
    . ::: :: :.: ::::  :. :. . : :.:: :  :  :::::.: .:: : ....:::
N-  SKPGTYVMTVTAIDADDP-NALNGMLRYRILSQAPSTPSPNMFTINNETGDIITVAAGLD

E-  RESYPTYTLVVQAADLQGE---GLSTTAKAVITVKDINDNAP
    ::.   :::.:::.:.:.   :::.:: ::::: :.::: :
N-  REKVQQYTLIIQATDMEGNPTYGLSNTATAVITVTDVNDNPP
```

Figure 4: Neural- and epithelial cadherin sequence comparison via LALIGN. Aligned sequences are shown with two dots designating alike residues and a single dot representing a similar amino acid based on charge, structure, hydrophobicity, etc.

FIGURE 5:

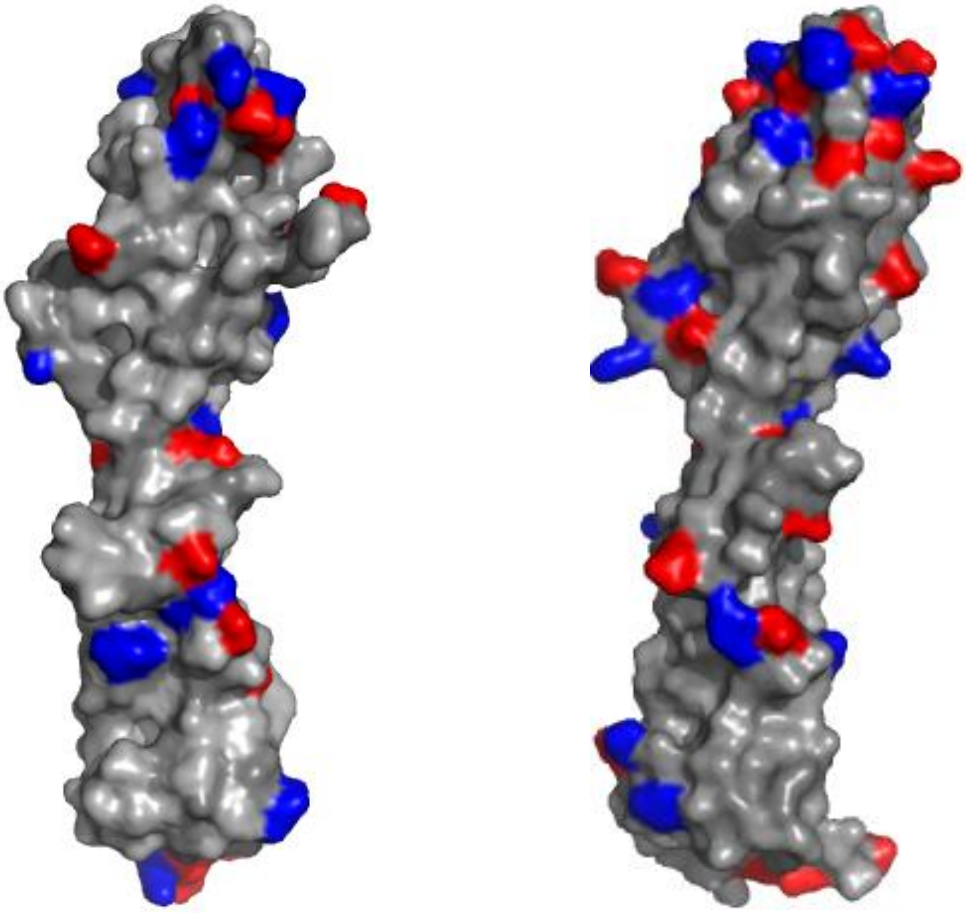

Figure 5: NCAD12 (left) and ECAD12 (right) displayed with titratable residues highlighted. Acidic residues are shown in red while basic residues are shown in blue. Clustering of titratable residues are specific locations on both proteins allow for the electrostatic tuning mechanism shown by NCAD12 results as well as possible hypotheses for future work on ECAD12.

FIGURE 6:

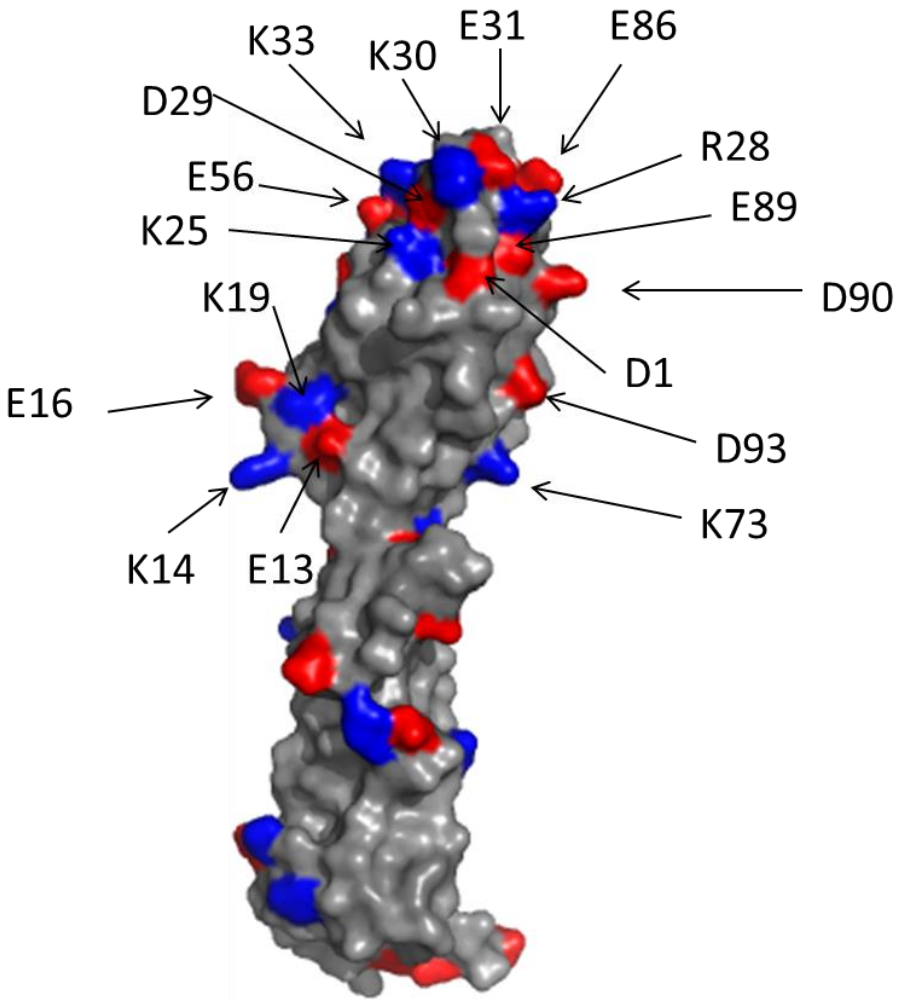

Figure 6: ECAD12 is shown with highlighted titrabable amino acid residues. Residues highlighted are all titrabable residues in EC1.

VITA

EDUCATION

2007- BA in Biochemistry- University of Mississippi